

Discovery of a Novel Aminopeptidase N Inhibitor Dino-Leucine Borate

Yuqian Ma^{1*}, Minzhi Fang^{2*}, Yutian Li¹, Dongqi Zhu¹, Yanmei Du¹, Binbin Ge¹, Jiliang Song¹, Xinyue Xu¹, Chuhan Ma¹, Xiaojun Jia¹, Xiurong Zhang¹, Jian Zhang¹, Dexiu Wang³, Xuejian Wang^{1#}

¹School of Pharmacy, Weifang Medical University, Weifang, China

²School of Basic Medicine, Weifang Medical University, Weifang, China

³School of Clinical Medicine, Weifang Medical University, Weifang, China

Email: #wangxuejian@wfmuc.edu.cn

How to cite this paper: Ma, Y.Q., Fang, M.Z., Li, Y.T., Zhu, D.Q., Du, Y.M., Ge, B.B., Song, J.L., Xu, X.Y., Ma, C.H., Jia, X.J., Zhang, X.R., Zhang, J., Wang, D.X. and Wang, X.Y. (2022) Discovery of a Novel Aminopeptidase N Inhibitor Dino-Leucine Borate. *Journal of Biosciences and Medicines*, 10, 150-168.

<https://doi.org/10.4236/jbm.2022.105014>

Received: April 8, 2022

Accepted: May 27, 2022

Published: May 30, 2022

Copyright © 2022 by author(s) and Scientific Research Publishing Inc.

This work is licensed under the Creative Commons Attribution International License (CC BY 4.0).

<http://creativecommons.org/licenses/by/4.0/>



Open Access

Abstract

Aminopeptidase N (APN/CD13), a Zn²⁺-dependent ectopeptidase localized on the cell surface, is widely considered to influence the invasion of tumor cells. We found that boroleucine and dino-leucine borate exhibited a strong inhibitory effect on the enzyme activity of aminopeptidase N. The tested assay indicated that both compounds had an anti-proliferative effect on triple-negative breast cancer cells. Wound healing assay, migration test and matrigel-coated transwell assay showed that both boroleucine and dino-leucine borate inhibited the migration and invasion of breast cancer cells. Immunoblot analysis showed that both compounds down-regulated the expression of matrix metalloproteinase-2/9. In the capillary tube formation assay of human umbilical vein endothelial cells (HUVECs), dino-leucine borate showed better antiangiogenic activity than ubenimex even at a low concentration (10 μM). Moreover, compared with ubenimex, the anti-metastatic activity of dino-leucine borate *in vivo* was similar to or even better than that of ubenimex in the H22 pulmonary metastasis mouse model. In this paper, we found the novel APN inhibitors to markedly suppress the enzyme activity of APN and inhibit the migration and invasion of tumor cells *in vitro* and *in vivo*.

Keywords

Aminopeptidase Inhibitor, Anti-Tumor, Boroleucine, Dino-Leucine Borate

1. Introduction

Aminopeptidase N (also known as CD13), a Zn²⁺ dependent membrane-bound

*These authors contributed equally to this work.

#Corresponding author.

ectopeptidase that is widely expressed in mammalian cells, has been associated with different aspects of normal (e.g. myeloid progenitor cells) as well as malignant development [1]. In addition, being a member of the M1 zinc metallopeptidase family, APN plays a crucial role in a variety of functions such as migration, invasion, angiogenesis, and metastasis of tumor cells [2]. Moreover, CD13 has been described as a functional biomarker of angiogenesis and surface marker of semi-dormant liver cancer stem cells (CSCs) in human liver cancer cells [3] [4] [5]. Scientists from Osaka University [6] found that CD13 is also a potential therapeutic target for liver cancer. Compared with the CD13 low group, the CD13 high group has earlier recurrence and shorter survival time, and CD13 enrichment is associated with early recurrence and poor prognosis in hepatocellular carcinoma (HCC) patients.

Aminopeptidase N is often overexpressed in tumor cells and is associated with angiogenesis and cancer progression. Guzmrojas *et al.* [5] compared the effects of APN deficiency in allografted malignant and non-malignant tumor cells on tumor growth and metastasis in mice, and found that APN activity in tumor and host cells jointly promoted tumor angiogenesis and growth in two independent tumor transplantation models. Therefore, it is important to find new CD13 inhibitors. At present, the only medicine as an APN inhibitor on the market is ubenimex, N-[(2S,3R)-3-amino-2-hydroxy-4-phenylbutanoyl]-L-leucine, also named Bestatin. Ubenimex was first marketed in Japan in 1987, and is often used as an adjuvant for immune enhancers in the treatment of leukemia or other anti-cancer drugs [7]. In recent years, studies have found that ubenimex has a good application prospect in the treatment of solid tumors, which can inhibit gastric cancer, non-small cell lung cancer, and colon cancer to a certain extent and prolong the survival of patients [8] [9] [10] [11].

Boroleucine((S)-1-amino-3-methyl-butylborate) and dino-leucine borate ((S)-1-amino-3-methyl-butylborate pinnae diol ester) are α -aminoborate derivatives, which are effective aminopeptidase inhibitors to suppress the enzyme activity of enkephalinase (EC 3.4.24.11) [12] and are often used as drug adjuvants. The inhibitory effect of ubenimex on leucine enkephalin metabolism was much weaker than that of boroleucine [13] [14]. According to the chemical structure of boroleucine and dino-leucine borate, we think they also can suppress the enzyme activity of APN (EC 3.4.11.2)? Therefore, these compounds have attracted our attention as APN inhibitors.

Breast cancer is the most common cancer and the leading cause of cancer death among females worldwide [15] [16]. Breast cancer treatment involves a multidisciplinary approach, such as traditional drug therapy, surgery, and radiation therapy. Effective breast cancer treatment requires maximum therapeutic effect with minimal adverse effects to ensure a good quality of life for patients [17] [18]. The common treatment is to give chemical medicine to patients, which can kill tumor cells and significantly improve the survival rate of patients. Therefore, it is important to find new effective APN inhibitors with small side effects. In this study, we found a new lead compound as an APN inhibitor that

has good anti-tumor activity. The results showed that boroleucine and di-no-leucine borate markedly suppressed the enzyme activity of APN and migration, invasion, and metastasis of tumor cells *in vitro* and *in vivo*. Therefore, the compound can be used as a lead compound for new drug development.

2. Materials and Methods

2.1. Cell Culture

Human K562 myeloid lymphoblastoma cell, human breast cancer cells MDA-MB-231 and MDA-MB-468 were obtained from the Cell Bank of Shanghai (Shanghai, China) and maintained in Roswell Park Memorial Institute (RPMI)-1640 supplemented with 10% fetal calf serum. The cells were incubated at 37°C in a humidified atmosphere containing 5% CO₂.

2.2. Molecular Dynamic Simulation

The molecular docking process was performed by Glide (schrodinger Inc, supported by Shanghai Institute of Materia Medica Chinese Academy of Sciences). The crystal structure of APN (PDB Entry: 2DQM) was chosen as the receptor in the docking study. Structural modifications were performed to make the protein suitable for docking. Water molecules and ligands crystallized in the protein structure were removed. OPLS 2005 force field was assigned to the refined structure. The structure of molecule 1 and 2 were sketched by maestro and prepared by LigPrep. The active site was defined as a cubic box containing residues at a distance of 20 Å around the ligand ubenimex.

2.3. Immunoblotting Analysis

The cells were lysed in RIPA lysis buffer containing protease inhibitor cocktail (Sigma–Aldrich) for 30 min on ice. Protein concentration was measured using a BCA protein assay kit (Beijing Solarbio Science and Technology). Then 30 µg protein was electrophoresed, separated in SDS-PAGE and transferred onto polyvinylidene difluoride (PVDF) membrane (Millipore). Target protein was determined by immunoblotting with their respective specific antibody. β -actin was used as internal control. Blots were visualized by an enhanced chemiluminescence kit (Millipore). Densitometry of immunoblotting was performed using AlphaEaseFC-v4.0.0 software. The following antibodies were used in this study: MMP-2 (dilution of 1:1000, catalog number sc-10736; Santa Cruz Biotechnology, China), MMP-9 (dilution of 1:1000, catalog number sc-21733; Santa Cruz Biotechnology, China) and β -actin (dilution of 1:5000, catalog number sc-1616; Santa Cruz Biotechnology).

2.4. Enzyme Activity Screening Assay

The activity of APN enzyme was detected by spectrophotometry using L-leucine-p-nitroanilide as an APN substrate. Monoclonal K562-APN cells (K562 cells with APN overexpression) were disrupted with ultrasonication in phosphate buf-

fer saline (PBS). After centrifugation (1000 g, 10 min), cell precipitate was discarded, and the supernatant was seeded into 96-well plates as enzyme source. Then different compounds were added to wells for 10 min. L-leucine-p-nitroanilide substrate was added into each well (1.2 mM). After incubation for 30 min, the enzyme activity was estimated by measuring the absorbance at 405 nm. The inhibition rate of compound was calculated by the following formula $(OD_{\text{control}} - OD_{\text{test}})/OD_{\text{control}} \times 100\%$ [8].

2.5. K_i Value Determination

30 μL phosphate buffer solution was added to the 96-well plate, followed by 10 μL compound and enzyme solution with different concentrations. After 5 min of incubation, 50 μL substrate and buffer solution was added and incubated at 37°C. Shake the plate quickly and thoroughly. The enzymatic reaction curve was measured at 405 nm for 15 min, and the absorbance value was measured every 1 min. The inhibition type was determined by Lineweaver-Burk mapping. The inhibition constant was determined by a second plot of K_m/V_{app} and the inhibitor concentration.

2.6. EdU Assay

The MDA-MB-231 and MDA-MB-468 cells were seeded at a density of 5×10^3 cells/well in 96-well plates. The EdU kit (cat. C0088L; Beyotime Institute of Biotechnology, Shanghai, China) was used to detect cell proliferation according to the manufacturer's instruction. The cells were treated with drugs for 48 h or 72 h, then washed with PBS, and incubated with 10 μM EdU in culture medium at room temperature for 2 h. The resulting absorbance was measured at 450 nm on a spectrophotometer. Each treatment was performed in triplicate wells per experiment.

2.7. Colony-Formation Assay

3000 cells/2ml/well MDA-MB-231 or MDA-MB-468 cells were put into six-well plate. After 12 h of seeding, cells were treated with drugs. Until each colony had more than 50 cells, then the experiment terminated. Washed twice with PBS and fixed with methanol for 10 min. Then cells were stained with 1% crystal violet for 5 min. Finally, colonies were washed with PBS and the photographs were captured under a microscope (IX81, Olympus).

2.8. Migration Assay

Breast cancer cells, treated with different compounds (20 μM), were plated in 6-well plates and incubated at 37°C, 5% CO_2 for 2 d. Then a line was drawn by the tip of 10 μL pipette and washed by PBS. The images of migrating cells were taken at 0 h and 24 h respectively. The experiment was repeated three times.

2.9. Invasion Assay

Breast cancer cell invasion assay was performed using transwell chamber

(transwell, 8 μm pore size; Corning Inc, Corning, New York, USA). The matrigel (Cat.356234; BD Biosciences, California, USA) was diluted with serumfree RPMI-1640 at 1:10, and 50 μL solution was added to the upper membrane for 2 h. Then 500 μL medium containing 1% FBS was added to the lower chamber. The cells (1×10^5 cells/well), pretreated with different compounds (20 μM) for 2 d, were plated into the upper chamber and incubated at 37°C for 24 h. Then the matrigel on the upper membrane was wiped. The invaded cells were fixed with methanol and stained with 5% crystal violet dye. The pictures were taken with a microscope (IX81; Olympus, Japan). The experiment was repeated three times.

2.10. HUVEC Tubular Structure Formation Assay

M199 medium (50 μL) and matrigel (50 μL) were added into 96-well plates for 0.5 h at 37°C. Add 100 μL compound (10 μM) and 50 μL cell suspension (20,000 cell/50 μL /well) and incubated at 37°C for 20 h. Images of five random fields per well were analyzed by Motic Image Plus 2.0 software (Motic Instruments Inc., Canada). The numbers of branch points of the formed tubes were counted and the average numbers were calculated. The experiments were repeated three times.

2.11. *In Vivo* Mouse H22 Pulmonary Metastasis Model

Four-week-old male Kunming mice were purchased from Hunan SJA Laboratory Animal Company (Hunan, China) and fed under specific pathogen-free conditions. To establish H22 pulmonary metastasis model, H22 cells (5×10^6) were suspended in 0.2 mL PBS and injected via tail vein on day 1. The mice were randomly divided into treatment and control group. Animal concentration is proposed to be 20 or 50 mg/kg/d based on previous data (data not shown). The treatment groups were injected intraperitoneally with 20 mg/kg/d or 50 mg/kg/d compounds respectively. The control group received an equal volume of PBS intraperitoneally from day 1 to day 15. The body weight was monitored every two days. On the 16th day, animals were sacrificed and the lungs were removed and fixed with Bouin's solution. The metastasis nodes on the surface of pulmonary lobes were counted. All animal experiments were approved by the Guidelines of the Animal Care and Use Committee of Weifang Medical University. All studies were performed in accordance with the National Institutes of Health (NIH) Guide for the Care and Use of Laboratory Animals (No. 8023, revised in 1978).

2.12. Statistical Analyses

All statistical analyses were performed using SPSS 17.0 statistical software package. Quantitative data was presented as mean \pm SEM. Statistical analysis was performed by one-way analysis of variance. For data of migration and invasion assay, significant difference between groups was performed by Student's t-test. $P < 0.05$ was considered statistically significant in all experiments.

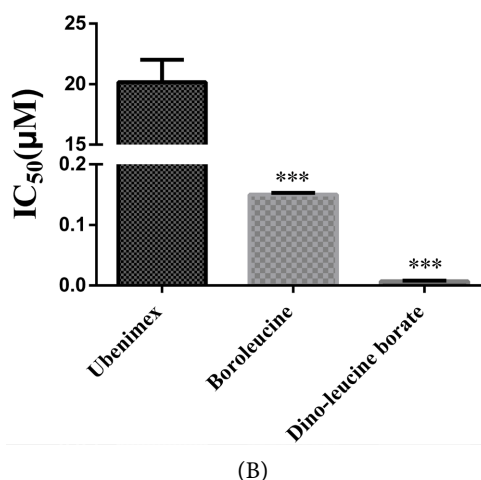
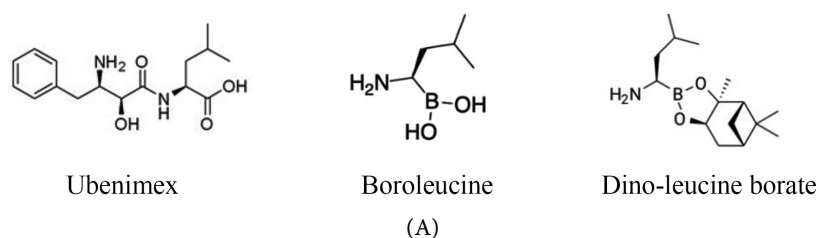
3. Results

3.1. Boroleucine and Dino-Leucine Borate Effectively Suppress APN Enzyme Activity

According to the chemical structure of boroleucine and dino-leucine borate, two compounds may suppress the enzyme activity of APN. Therefore, we employed a method to detect the effect of two compounds on suppressing homosapien APN enzyme activity, as we previously reported [19]. The enzyme suppression IC_{50} of ubenimex, boroleucine and dino-leucine borate was 20.17 μ M, 0.15 μ M, 0.007 μ M, respectively (Figure 1(A), Figure 1(B)). This data suggested that boroleucine and dino-leucine borate have better suppression effect on APN enzyme activity than ubenimex.

The IC_{50} value may vary between different laboratories, K_i is a parameter to a compound. Then we detected K_i of three compounds. Using Lineweaver-Burk double reciprocal plots, a series of straight lines intersected in the second quadrant indicated that three compounds belong to competitive inhibition type. K_i value of ubenimex, boroleucine, and dino-leucine borate were 18.78 μ M, 1.73 μ M, 0.77 μ M, respectively (Figure 1(C)). This result also indicated that boroleucine and dino-leucine borate strongly combine with APN enzyme.

According to the chemical structure of dino-leucine borate, it is unstable and may degrade to boroleucine. In order to verify this hypothesis, we placed boroleucine and dino-leucine for several days to measure the inhibition rate of APN enzyme activity. The inhibition rate of boroleucine was only 4.3% on the first day and decreased slowly over time. However, the inhibition rate of dino-leucine borate was 68% on the first day and decreased rapidly over time to 0.27%, which



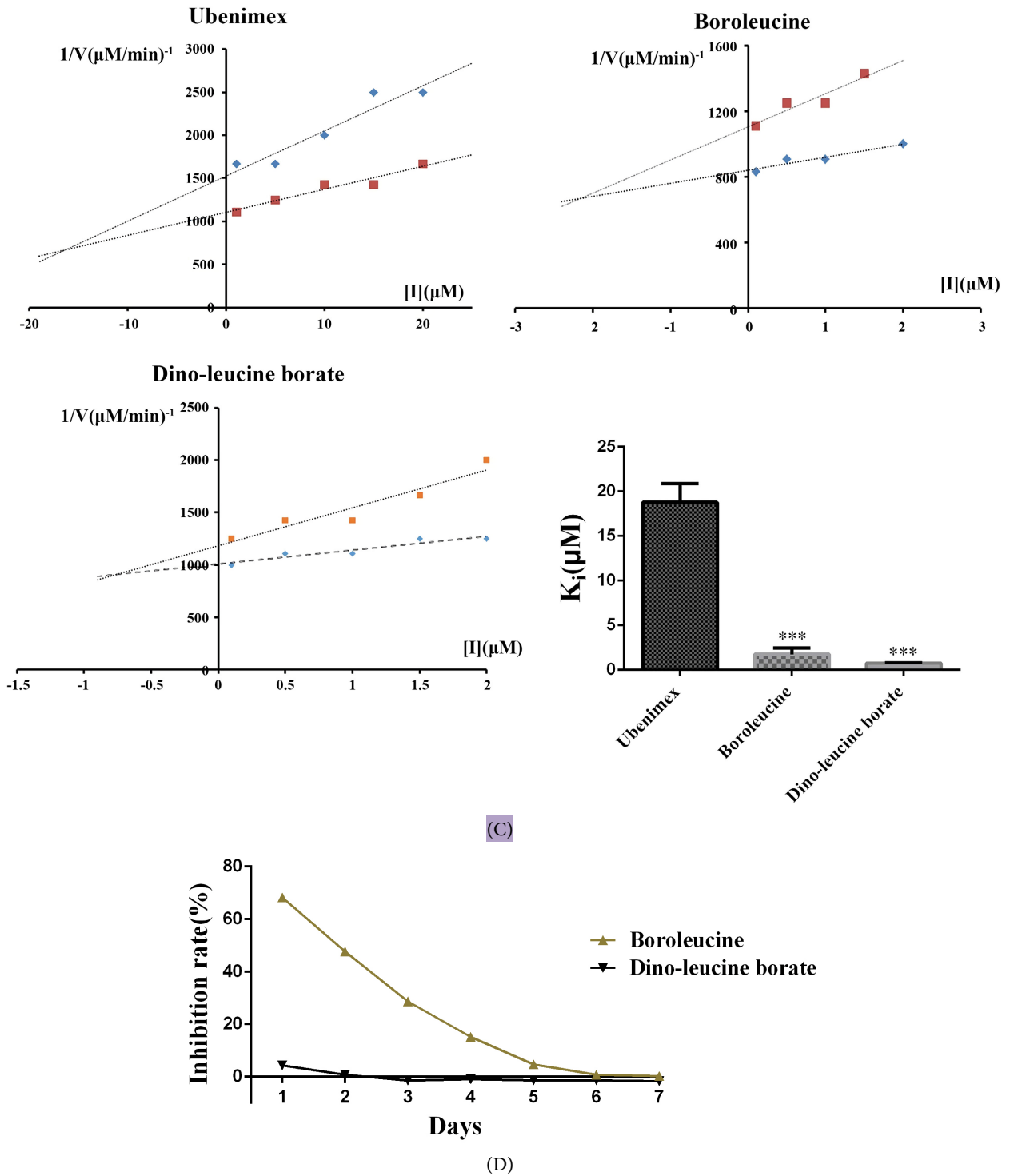


Figure 1. Boroleucine and Dino-leucine borate effectively suppress APN enzyme activity. (A) Chemical structure of ubenimex, boroleucine, and dino-leucine borate. (B) The APN enzyme activity was determined by measuring the absorbance at 405 nm, as the substrate was L-leucine p-nitroanilide hydrochloride, the IC_{50} of ubenimex, boroleucine and dino-leucine borate were obtained. Data are presented as mean \pm SEM. ** $p \leq 0.01$, *** $p \leq 0.001$. (C) Compound and aminopeptidase N enzyme solution were mixed with substrate and buffer, and incubated at 37°C. The enzymatic reaction curve was measured every 1min for 15 min at 405 nm. The K_i value of three compounds was calculated. Data are presented as mean \pm SEM. ** $p \leq 0.01$, *** $p \leq 0.001$. (D) 10 nM of boroleucine and dino-leucine borate were placed at room temperature for several days. Then the APN enzyme activity inhibition was measured.

was as same as that of boroleucine (Figure 1(D)). Therefore, we think that the degradation product of dino-leucine borate is boroleucine, and dino-leucine borate can convert into boroleucine over time.

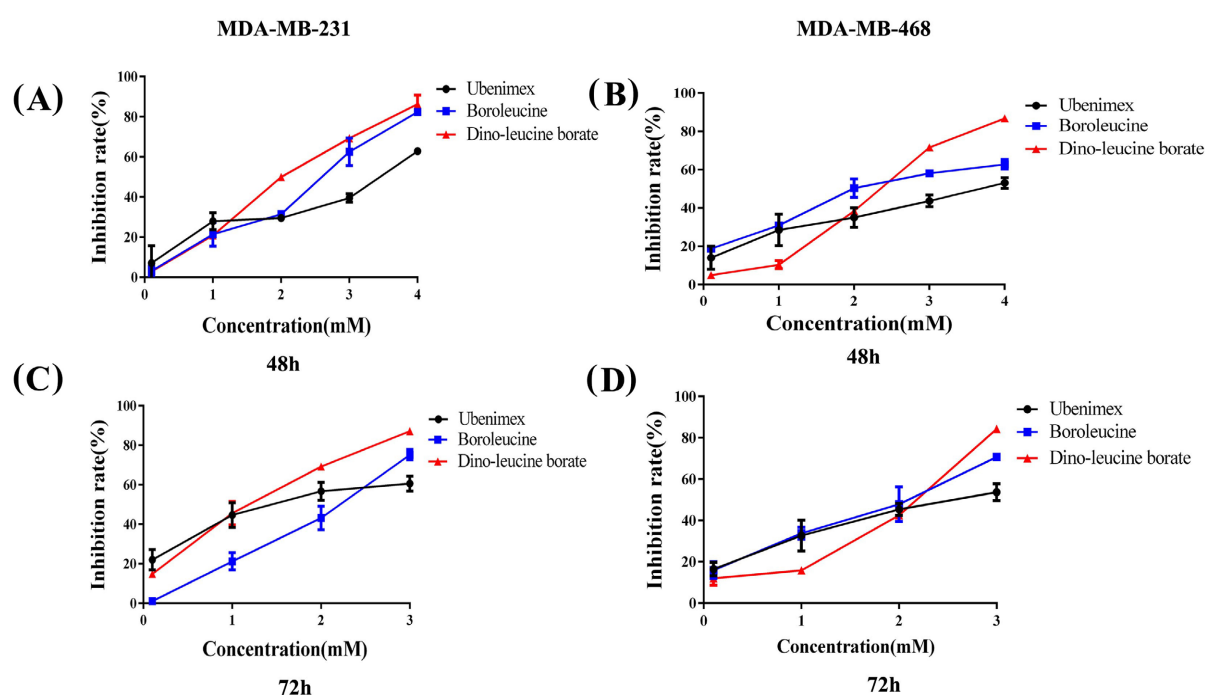
3.2. Boroleucine and Dino-Leucine Borate Inhibit the Proliferation of MDA-MB-231 and MDA-MB-468 Cells

To test the effect of compound on cell proliferation, we performed EdU assay. The data suggested that ubenimex, boroleucine, and dino-leucine borate had little effect on cell proliferation in MDA-MB-231 and MDA-MB-468 cells when concentration was 1 mM. (Figures 2(A)-(D)) According to other data (Data not shown), we chose 20 μ M to do the following test. At this concentration, three compounds rarely inhibited the proliferation of tumor cells. Therefore, the concentration of 20 μ M was selected to treat cells in wound healing, migration and trans-well invasion assay.

Colony-formation assay is an effective method to determine the proliferation ability of single cell *in vitro*. Therefore, we evaluated the effect of boroleucine, dino-leucine borate, and ubenimex on the colony formation ability in triple negative breast cancer cells. We found that all compounds inhibited colony formation, and boroleucine had the same inhibitory effect as ubenimex. However, dino-leucine borate had a stronger inhibitory effect than ubenimex on colony formation (Figure 2(E), Figure 2(F)).

3.3. Boroleucine and Dino-Leucine Borate Inhibit the Migration and Invasion of Breast Cancer Cells and Downregulate the Expression of Metastasis-Related Proteins

The effects of boroleucine and dino-leucine borate on migration and invasion of



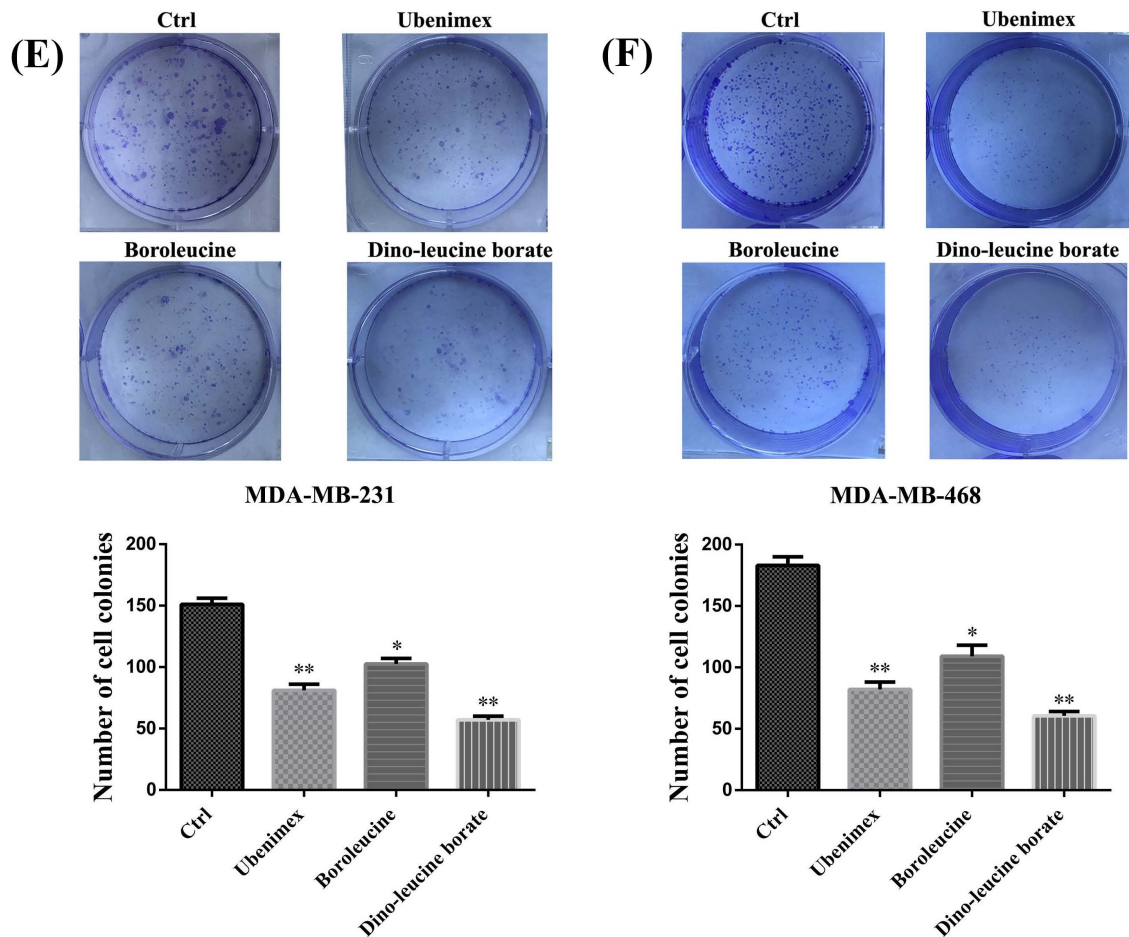
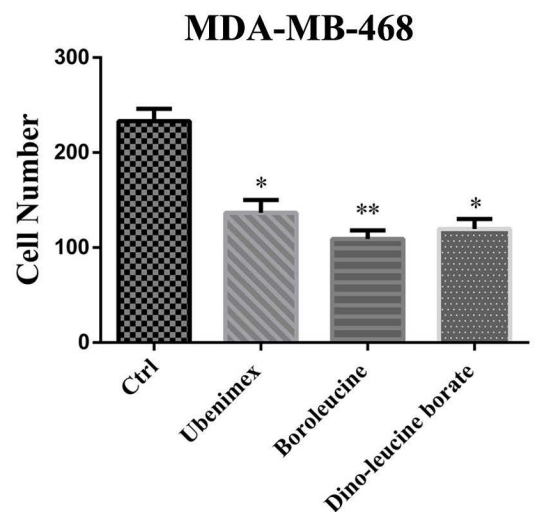
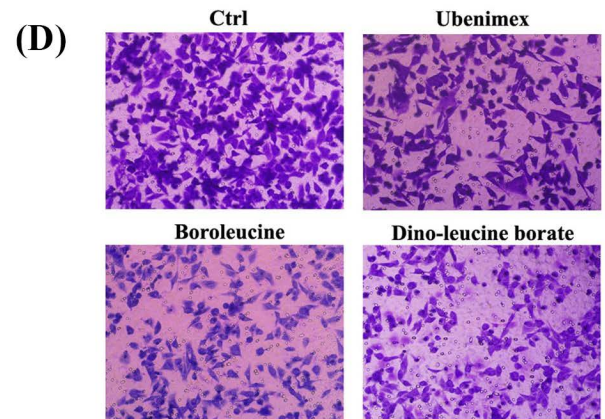
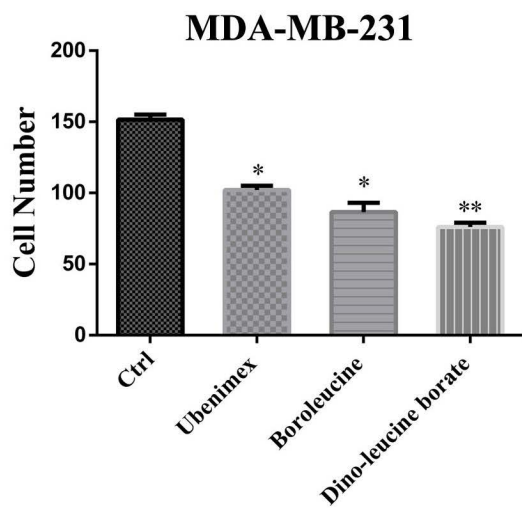
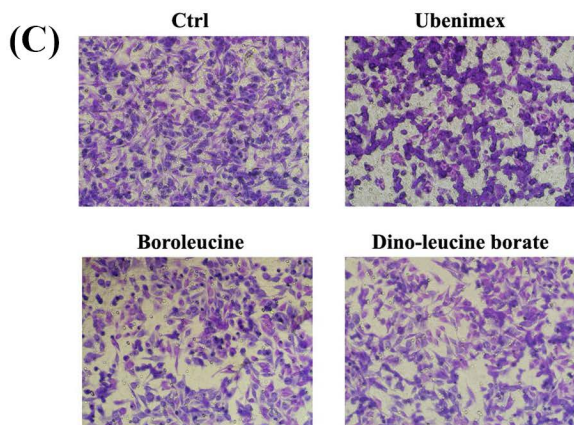
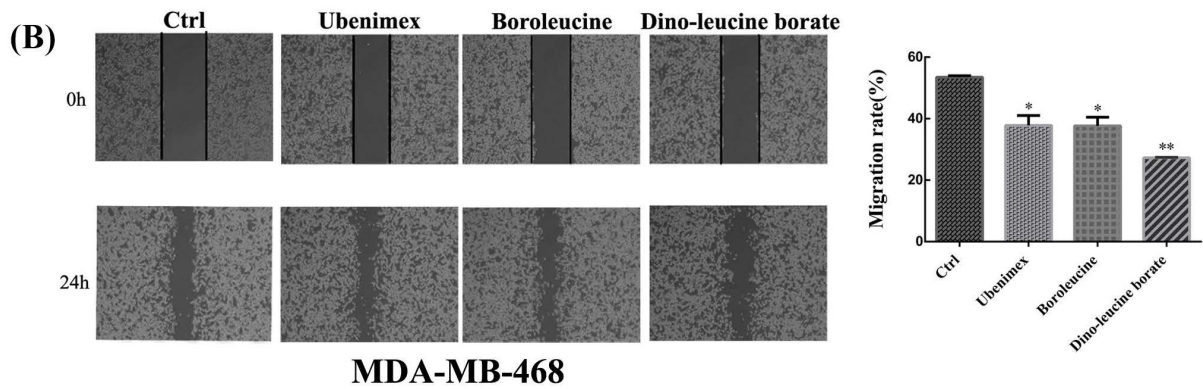
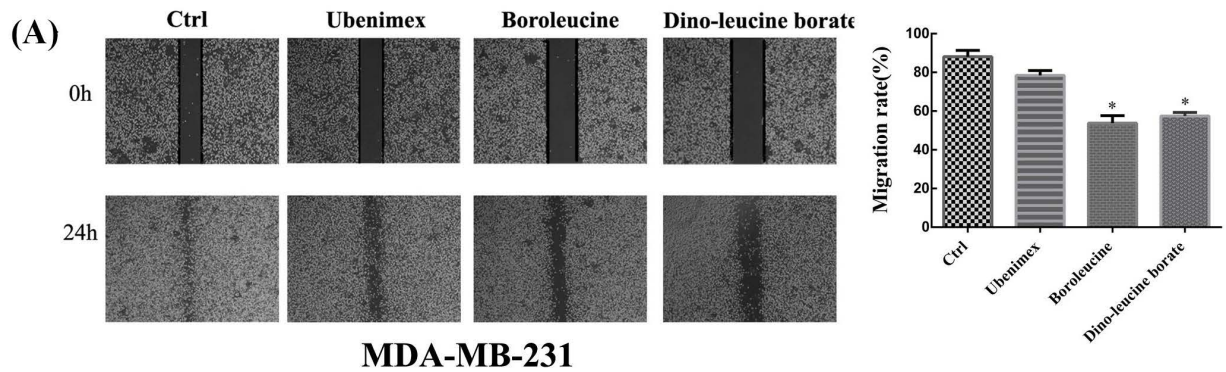


Figure 2. Boroleucine and Dino-leucine borate inhibit the proliferation of MDA-MB-231 and MDA-MB-468 cells. (A-D) MDA-MB-231 and MDA-MB-468 cells were treated with ubenimex, boroleucine, and dino-leucine borate for 48 h or 72 h. EdU assay was used to detect cell proliferation. (E-F) The sensitivity of cells to ubenimex, boroleucine, and dino-leucine borate was tested by colony-formation assay. Data are presented as mean \pm SEM. * $p \leq 0.05$, ** $p \leq 0.01$.

MDA-MB-231 and MDA-MB-468 cells were tested. The wound healing assay showed that boroleucine and dino-leucine borate had a stronger inhibitory effect on cell migration than ubenimex in MDA-MB-231 cells after 24 h treatment. This suppression effect was also verified in MDA-MB-468 cells at the same condition (**Figure 3(A)**, **Figure 3(B)**). We also employed transwell migration assay without matrigel to test cell migration. The results showed that the number of trans-membrane cells in the three compound groups was significantly reduced compared with Ctrl group. While the inhibitory effect of boroleucine and dino-leucine borate was better than that of ubenimex. The inhibitory effect of boroleucine and dino-leucine borate on cell migration was also verified in MDA-MB-468 cells at the same condition (**Figure 3(C)**, **Figure 3(D)**).

Then, human umbilical vein endothelial cells (HUVECs) tubular structure formation assay was used to evaluate the anti-angiogenesis activity. The results showed that dino-leucine borate significantly reduced the capillary tube formation compared with ubenimex (**Figure 3(E)**).



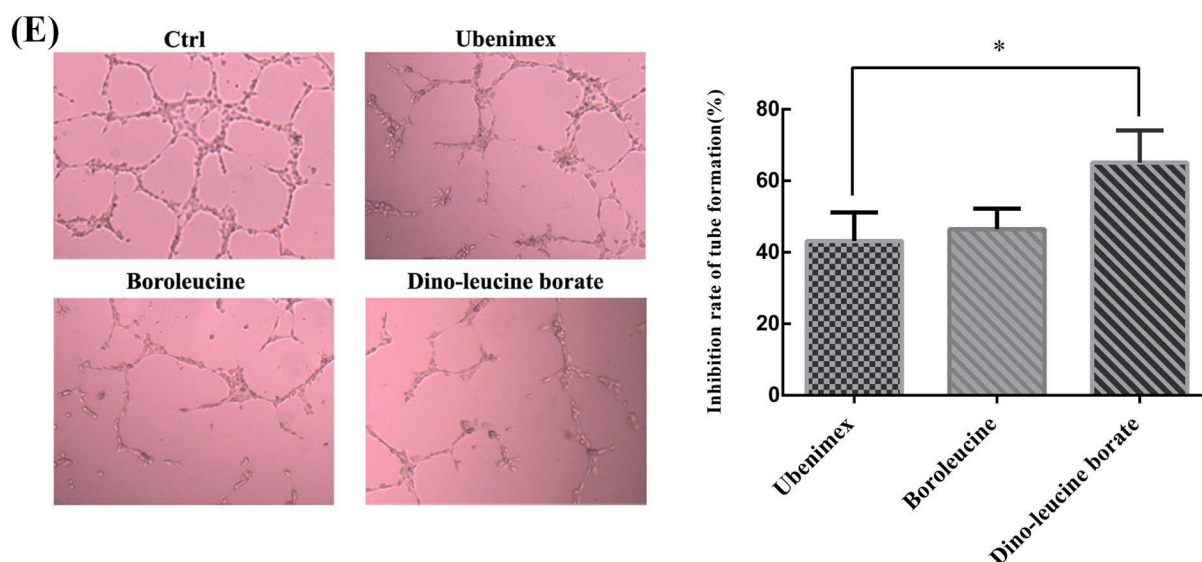
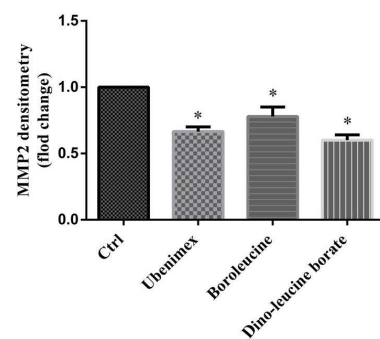
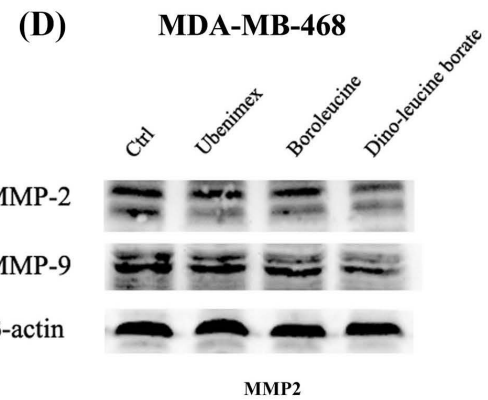
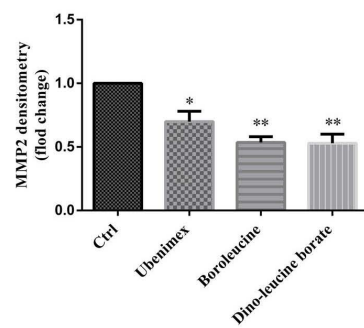
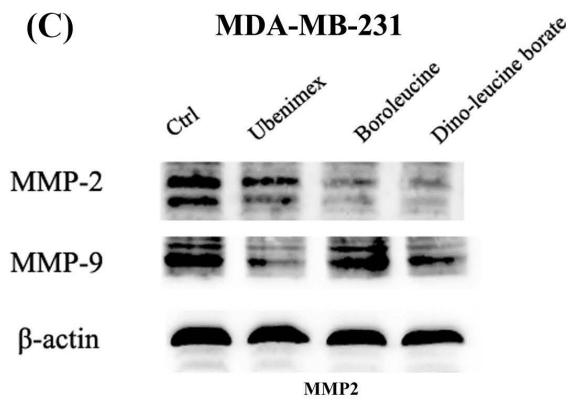
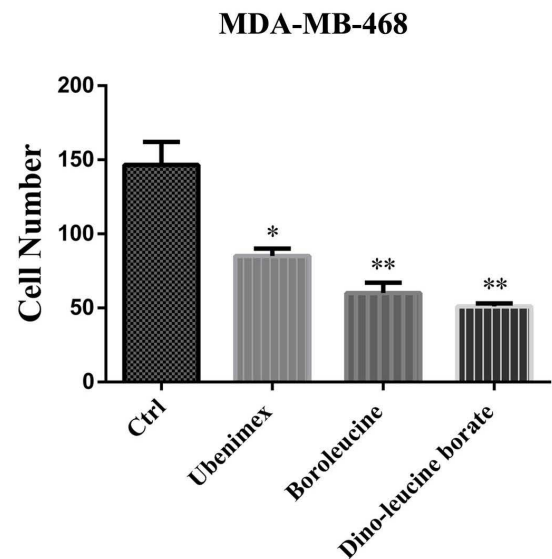
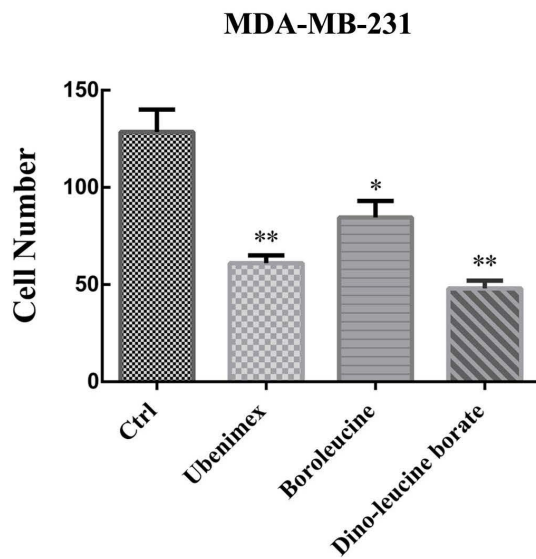
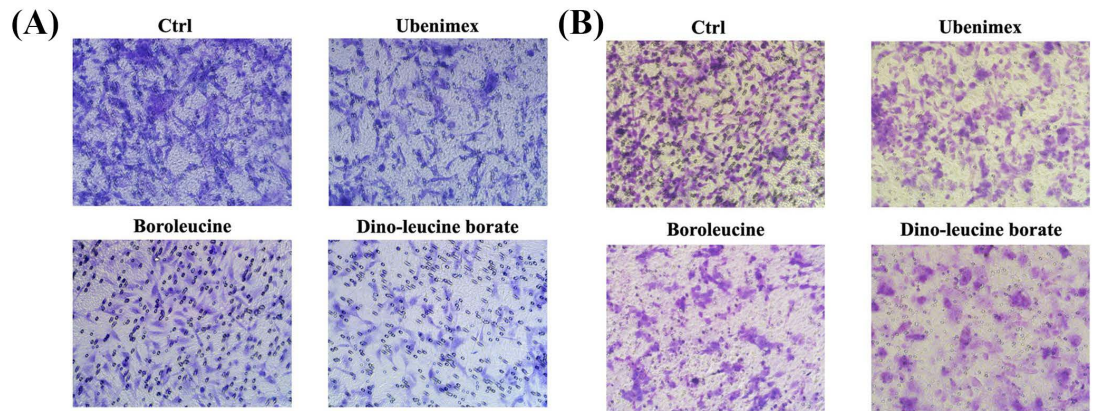


Figure 3. Boroleucine and dino-leucine borate inhibit the migration of breast cancer cells and HUVECs tubular structure formation. (A-B) MDA-MB-231 and MDA-MB-468 cells were treated with ubenimex, boroleucine, and dino-leucine borate for 2 d. Then the cells were wounded by a 20 μ l pipette tip and photographed at 0 and 24 h. Data are presented as mean \pm SEM. * $p \leq 0.05$, ** $p \leq 0.01$. (C-D) MDA-MB-231 and MDA-MB-468 cells, pretreated with ubenimex, boroleucine, and dino-leucine borate for 2 d, were plated into transwell chambers and photographed (200 \times) after 24 h in transwell migration assay. The data represented the mean number of migrated cells from five different fields. Data are presented as mean \pm SEM. * $p \leq 0.05$, ** $p \leq 0.01$. (E) HUVEC cells were plated on matrigel in 96-well plates, and then treated with 20 μ M of three compounds for 20 h. Photographs were taken using an invert microscope (200 \times). Data are presented as mean \pm SEM. * $p \leq 0.05$, ** $p \leq 0.01$.

Boroleucine and dino-leucine borate inhibited the invasion of MDA-MB-231 cells in transwell assay coating with matrigel, and dino-leucine borate's inhibitory effect was better than that of ubenimex. Their inhibitory effect was also verified in MDA-MB-468 cells at the same condition (Figure 4(A), Figure 4(B)), while the effect of three compounds on the expression of MMP-2/9 were detected. WB result showed that all three compounds down-regulated the expression of MMP-2/9 at 20 μ M. Moreover, the downregulation effect of dino-leucine borate was more potent than that of boroleucine and ubenimex (Figure 4(C), Figure 4(D)). These results together suggested boroleucine and dino-leucine borate inhibit migration and invasion of tumor cells.

3.4. Ubenimex, Boroleucine, and Dino-Leucine Borate Inhibit Lung Metastasis in Kunming Mice Bearing Hepatocellular Carcinoma H22 Cells

Based on the significant role of APN in tumor metastasis, we used *in vivo* H22 pulmonary metastasis model to evaluate the anti-metastasis activity of three compounds. The number of metastatic pulmonary node was counted. As depicted in Figure 5, the number of node in mice treated with dino-leucine borate (20 mg/kg, ip) was lower than that of ubenimex group (20 mg/kg, ip) (Figure 5(A)). The pulmonary node number of dino-leucine borate and ubenimex were 16 and 28, respectively. There were no apparent loss of body weight and no evident toxic



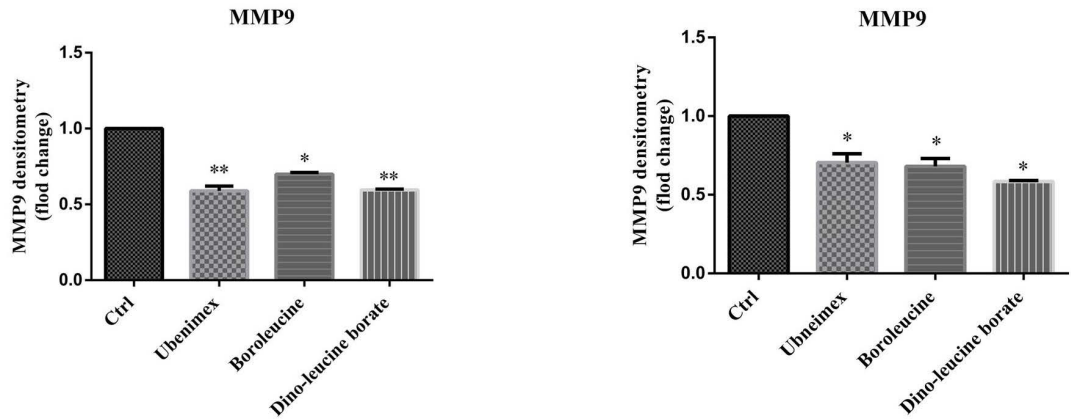
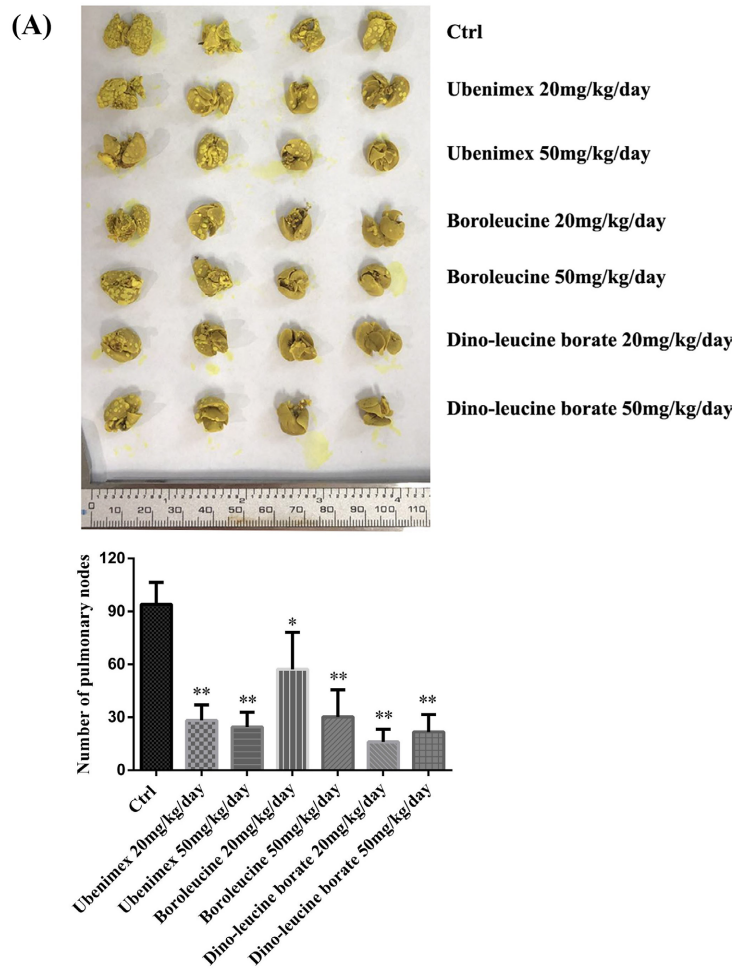


Figure 4. Boroleucine and dino-leucine borate inhibit invasion of breast cancer cells and downregulate the expression of metastasis-related proteins. (A-B) MDA-MB-231 and MDA-MB-468 cells, pretreated with ubenimex, boroleucine, and dino-leucine borate for 2 d, were plated into matrigel-coated transwell chambers and photographed (200×) after 24 h in invasion assay. The data represented the mean number of invaded cells from five different fields. Data are presented as mean ± SEM. * $p \leq 0.05$, ** $p \leq 0.01$. (C-D) MDA-MB-231 and MDA-MB-468 cells were treated with ubenimex, boroleucine, and dino-leucine borate for 2 d. The expression level of MMP-2/9 was detected by immunoblotting. Actin was the protein loading control. A representative immunoblot from three independent experiments giving similar results is shown for each western blot experiment. Data are presented as mean ± SEM. * $p \leq 0.05$, ** $p \leq 0.01$.



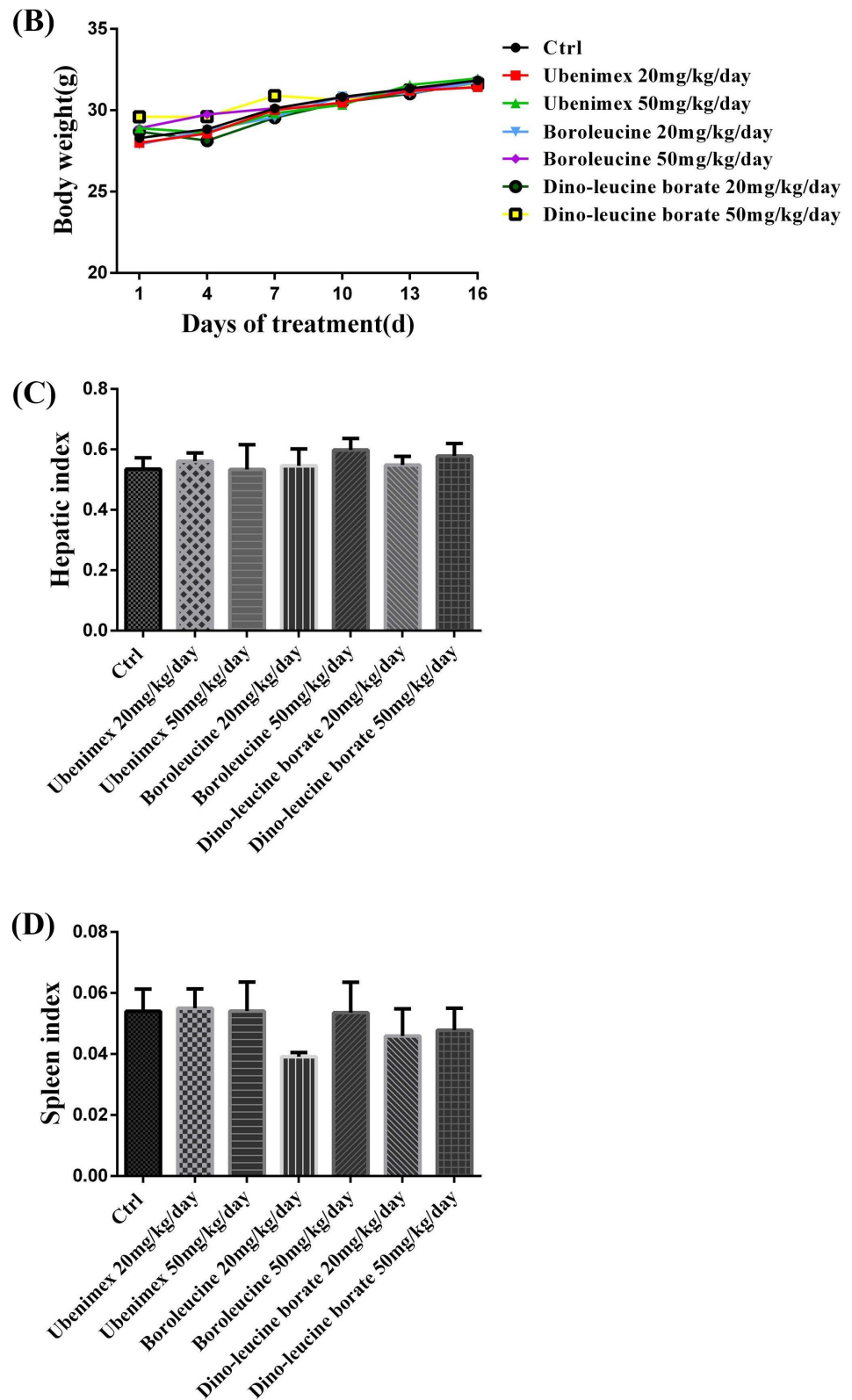


Figure 5. Anti-metastasis activity of boroleucine and dino-leucine borate was evaluated *in vivo*. (A) Lung metastasis node number in the H22 hepatoma pulmonary metastasis model. Data are presented as mean \pm SEM. * $p \leq 0.05$, ** $p \leq 0.01$. (B-D) Body weight, liver and spleen index of ubenimex, boroleucine, and dino-leucine borate groups.

catalytic site of APN and inhibit the enzyme activity *in vitro*. In addition, boroleucine and dino-leucine borate could not be detected by HPLC and HPLC-MS. Therefore, we proved that dino-leucine borate could be converted to boroleucine by the inhibition rate of APN activity. Compared with ubenimex, both compounds significantly delayed cell scratch healing and inhibited cell invasion of MDA-MB- 231 and MDA-MB-468 cells at a non-toxic dose. MMP2 and MMP9 are known to be closely related to the invasion and metastasis of cancer cells [22] [23]. In our study, we found that all three compounds significantly suppressed the expression of MMP2/9, and the down-regulation effect of dino-leucine borate was more potent than that of boroleucine and ubenimex. Meanwhile, dino-leucine borate demonstrated more potential anti-angiogenesis activity than ubenimex in the tubular structure formation assay of HUVECs. In addition, dino-leucine borate exhibited a promising anti-metastasis effect in the H22 pulmonary metastasis mouse model, which deserves further research and development as an anti-metastatic lead compound.

A large amount of evidence suggests that APN can be used as a promising marker for cancer diagnosis since APN is up-regulated in tumor cells and plays a vital role in tumor invasion, metastasis, and angiogenesis [24] [25] [26] [27] [28]. Therefore, a sensitive and selective method for *in situ* detection of APN expression is of great significance for the diagnosis and pathophysiological elucidation of APN-related disease. The results showed that both boroleucine and dino-leucine borate significantly inhibited the activity of APN. These compounds can be used as the forerunners of APN inhibitors in the development of new drugs, and can also be used to synthesize APN targeted fluorescent probes for the early detection of tumors.

APN-targeted fluorescent probe is used for the early detection of tumors. Li H [29]'s research group developed a novel two-photon near-infrared fluorescence probe DCM-APN, which can be used to trace APN *in vitro* and *in vivo*. The probe DCM-APN is used to distinguish normal cells from cancer cells, indicating that probe DCM-APN is an effective tool for detecting APN, and is helpful for the early diagnosis of tumours in clinical medicine. Hahnenkamp A [30] synthesized a non-peptide small molecule fluorescent imaging agent with a high affinity for APN. It plays a key role in pathophysiological angiogenesis. The low K_i values of boroleucine and dino-leucine borate also indicated that they combine strongly with APN and can be used to develop fluorescence probes for early detection of tumors through targeting APN.

This study has several limitations. For example, we only discussed the activity of two compounds and did not design experiments to prove their role *in vivo* imaging in mice or their toxic effects on normal cells. Our current research is still in the preliminary stage of searching for potent compounds. In future experiments, we will further study the anti-tumor mechanism of APN inhibitors. Above all, the two new structures of boroleucine and dino-leucine borate are expected to be used as lead compounds for the design and synthesis of new APN

inhibitor, and targeting APN for early tumor detection through developing new fluorescence probe.

Boroleucine and dino-leucine borate significantly inhibit the enzymatic activity of APN and inhibit the proliferation, migration and invasion of triple-negative breast cancer cells as well as lung metastasis *in vivo*, and can therefore be used as aminopeptidase N inhibitor class anti-tumour lead compounds for new drug development.

Author Contributions

Conception and design: Yuqian Ma, Minzhi Fang, Xuejian Wang;

Experiments and analyzed the data: Yuqian Ma, Yutian Li, and Dongqi Zhu;

Manuscript writing: Yuqian Ma, Minzhi Fang, Xuejian Wang;

Final approval of manuscript: All authors;

Accountable for all aspects of the work: All authors.

Acknowledgements

This work was supported by the National Natural Science Foundation of China (Grant No. 81503108 and 81803368), University Students Science and Technology Innovation Fund Project (X2021392), Shandong Traditional Chinese Medicine Science and Technology Project (2021Q071) and Weifang Science, and Technology Development Plan Project (2021YX044).

Data Availability

The datasets generated and analyzed during the current study are available from the corresponding author on reasonable request.

Conflicts of Interest

The authors declare that they have no conflict of interest.

References

- [1] Wickstrom, M., Larsson, R., Nygren, P. and Gullbo, J. (2011) Aminopeptidase N (CD13) as a Target for Cancer Chemotherapy. *Cancer Science*, **102**, 501-508. <https://doi.org/10.1111/j.1349-7006.2010.01826.x>
- [2] Amin, S.A., Adhikari, N. and Jha, T. (2018) Design of Aminopeptidase N Inhibitors as Anti-Cancer Agents. *Journal of Medicinal Chemistry*, **61**, 6468-6490. <https://doi.org/10.1021/acs.jmedchem.7b00782>
- [3] Pasqualini, R., Koivunen, E., Kain, R., Lahdenranta, J., Sakamoto, M., Stryhn, A., Ashmun, R., Shapiro, L., Arap, W. and Ruoslahti, E. (2000) Aminopeptidase N Is a Receptor for Tumor-Homing Peptides and a Target for Inhibiting Angiogenesis. *Cancer Research*, **60**, 722-727.
- [4] Haraguchi, N., Ishii, H., Mimori, K., Tanaka, F., Ohkuma, M., MinKim, H., Akita, H., Takiuchi, D., Hatano, H., Nagano, H., Barnard, G.F., Doki, Y. and Mori, M. (2010) CD13 Is a Therapeutic Target in Human Liver Cancer Stem Cells. *Journal of Clinical Investigation*, **120**, 3326-3339. <https://doi.org/10.1172/JCI42550>

- [5] Guzman-Rojas, L., Rangel, R., Salameh, A., Edwards, J.K., Dondossola, E., Yun-Gon, K., *et al.* (2012) Cooperative Effects of Aminopeptidase N (CD13) Expressed by Nonmalignant and Cancer Cells within the Tumor Microenvironment. *Proceedings of the National Academy of Sciences of the United States of America*, **109**, 1637-1642. <https://doi.org/10.1073/pnas.1120790109>
- [6] Yamanaka, C., Wada, H., Eguchi, H., Hatano, H., Gotoh, K., Noda, T., Yamada, D., Asaoka, T., Kawamoto, K., Nagano, H., Doki, Y. and Mori, M. (2018) Clinical Significance of CD13 and Epithelial Mesenchymal Transition (EMT) Markers in Hepatocellular Carcinoma. *Japanese Journal of Clinical Oncology*, **48**, 52-60. <https://doi.org/10.1093/jjco/hyx157>
- [7] Jiang, Y., Hou, J., Li, X., Huang, Y., Wang, X., Wu, J., Zhang, J., Xu, W. and Zhang, Y. (2016) Discovery of a Novel Chimeric Ubenimex-Gemcitabine with Potent Oral Antitumor Activity. *Bioorganic & Medicinal Chemistry*, **24**, 5787-5795. <https://doi.org/10.1016/j.bmc.2016.09.033>
- [8] Zhao, S., Yao, K., Li, D., Liu, K., Jin, G., Yan, M., Wu, Q., Chen, H., Shin, S.H., Bai, R., Wang, G., Bode, A.M., Dong, Z., Guo, Z. and Dong, Z. (2019) Inhibition of LTA4H by Bestatin in Human and Mouse Colorectal Cancer. *EBioMedicine*, **44**, 361-374. <https://doi.org/10.1016/j.ebiom.2019.05.008>
- [9] Ota, K. and Uzuka, Y. (1992) Clinical Trials of Bestatin for Leukemia and Solid Tumors. *Biotherapy*, **4**, 205-214. <https://doi.org/10.1007/BF02174207>
- [10] Kawai, Y. (2004) Gan to kagaku ryoho. *Cancer & Chemotherapy*, **31**, 678.
- [11] Yasumitsu, T., Ohshima, S., Nakano, N., Kotake, Y. and Tominaga, S. (1990) Bestatin in Resected Lung Cancer. A Randomized Clinical Trial. *Acta Oncologica*, **29**, 827-831. <https://doi.org/10.3109/02841869009093009>
- [12] Schwartz, J.C., Gros, C., Lecomte, J.M. and Bralet, J. (1990) Enkephalinase (EC 3.4.24.11) Inhibitors: Protection of Endogenous ANF against Inactivation and Potential Therapeutic Applications. *Life Sciences*, **47**, 1279-1297. [https://doi.org/10.1016/0024-3205\(90\)90192-T](https://doi.org/10.1016/0024-3205(90)90192-T)
- [13] Hussain, M.A., Rowe, S.M., Shenvi, A.B. and Aungst, B.J. (1990) Inhibition of Leucine Enkephalin Metabolism in Rat Blood, Plasma and Tissues *in Vitro* by an Aminoboronic Acid Derivative. *Drug Metabolism & Disposition*, **18**, 288-291.
- [14] Hussain, M.A., Koval, C.A., Shenvi, A.B. and Aungst, B.J. (1990) Recovery of Rat Nasal Mucosa from the Effects of Aminopeptidase Inhibitors. *Journal of Pharmaceutical Sciences*, **79**, 398-400. <https://doi.org/10.1002/jps.2600790507>
- [15] Siegel, R.L., Miller, K., Goding Sauer, A., Fedewa, S.A., Butterly, L.F., Anderson, J.C., Cercek, A., Smith, R.A. and Jemal, A. (2020) Colorectal Cancer Statistics 2020. *CA: A Cancer Journal for Clinicians*, **70**, 145-164. <https://doi.org/10.3322/caac.21601>
- [16] Winters, S., Martin, C., Murphy, D. and Shokar, N.K. (2017) Breast Cancer Epidemiology, Prevention, and Screening. *Progress in Molecular Biology and Translational Science*, **151**, 1-32. <https://doi.org/10.1016/bs.pmbts.2017.07.002>
- [17] Fisusi, F.A. and Akala, E.O. (2019) Drug Combinations in Breast Cancer Therapy. *Pharmaceutical Nanotechnology*, **7**, 3-23. <https://doi.org/10.2174/2211738507666190122111224>
- [18] Fahad Ullah, M. (2019) Breast Cancer: Current Perspectives on the Disease Status. *Advances in Experimental Medicine and Biology*, **1152**, 51-64. https://doi.org/10.1007/978-3-030-20301-6_4
- [19] Liu, H., Wang, X., Yang, H., Zhao, Y., Ji, P., Ma, H., Zhou, Y., Wang, Y., Zhang, H., Jiang, W., Fang, C., Feng, L. and Wang, X. (2019) New Method for Detecting the

- Suppressing Effect of Enzyme Activity by Aminopeptidase N Inhibitor. *Chemical and Pharmaceutical Bulletin (Tokyo)*, **67**, 155-158.
<https://doi.org/10.1248/cpb.c18-00667>
- [20] Ferlay, J., Soerjomataram, I., Dikshit, R., Eser, S., Mathers, C., Rebelo, M., Parkin, D.M., Forman, D. and Bray, F. (2015) Cancer Incidence and Mortality Worldwide: Sources, Methods and Major Patterns in GLOBOCAN 2012. *International Journal of Cancer*, **136**, E359-E386. <https://doi.org/10.1002/ijc.29210>
- [21] Siegel, R.L., Miller, K.D. and Jemal, A. (2017) Cancer Statistics, 2017. *CA: A Cancer Journal for Clinicians*, **67**, 7-30. <https://doi.org/10.3322/caac.21387>
- [22] Poudel, B., Kim, D.K., Ki, H.H., Kwon, Y.B. and Lee, Y.M. (2014) Down Regulation of RK Signaling Impairs U2OS Osteosarcoma Cell Migration in Collagen Matrix by Suppressing MMP9 Production. *Oncology Letters*, **7**, 215-218.
<https://doi.org/10.3892/ol.2013.1655>
- [23] Poudel, B., Lee, Y.M. and Kim, D.K. (2015) DDR2 Inhibition Reduces Migration and Invasion of Murine Metastatic Melanoma Cells by Suppressing MMP2/9 Expression through ERK/NF-kappa B Pathway. *Acta Biochimica et Biophysica Sinica (Shanghai)*, **47**, 292-298. <https://doi.org/10.1093/abbs/gmv005>
- [24] Cui, S.X., Qu, X.J., Gao, Z.H., Zhang, Y.S., Zhang, X.F., Zhao, C.R., Xu, W.F., Li, Q.B. and Han, J.X. (2010) Targeting Aminopeptidase N (APN/CD13) with Cyclic-Imide Peptidomimetics Derivative CIP-13F Inhibits the Growth of Human Ovarian Carcinoma Cells. *Cancer Letters*, **292**, 153-162.
<https://doi.org/10.1016/j.canlet.2009.11.021>
- [25] Fontijn, D., Duyndam, M.C., van Berkel, M.P., Yuana, Y., Shapiro, L.H., Pinedo, H.M., Broxterman, H.J. and Boven, E. (2006) CD13/Aminopeptidase N Overexpression by Basic Fibroblast Growth Factor Mediates Enhanced Invasiveness of 1F6 Human Melanoma Cells. *British Journal of Cancer*, **94**, 1627-1636.
<https://doi.org/10.1038/sj.bjc.6603157>
- [26] Tokuhara, T., Hattori, N., Ishida, H., Hirai, T., Higashiyama, M., Kodama, K. and Miyake, M. (2006) Clinical Significance of Aminopeptidase N in Non-Small Cell Lung Cancer. *Clinical Cancer Research*, **12**, 3971-3978.
<https://doi.org/10.1158/1078-0432.CCR-06-0338>
- [27] Mawrin, C., Wolke, C., Haase, D., Krüger, S., Firsching, R., Keilhoff, G., Paulus, W., Gutmann, D.H., Lal, A. and Lendeckel, U. (2010) Reduced Activity of CD13/Aminopeptidase N (APN) in Aggressive Meningiomas Is Associated with Increased Levels of SPARC. *Brain Pathology*, **20**, 200-210.
<https://doi.org/10.1111/j.1750-3639.2009.00267.x>
- [28] Petrovic, N., Schacke, W., Gahagan, J.R., O'Connor, C.A., Winnicka, B., Conway, R.E., Mina-Osorio, P. and Shapiro, L.H. (2007) CD13/APN Regulates Endothelial Invasion and Filopodia Formation. *Blood*, **110**, 142-150.
<https://doi.org/10.1182/blood-2006-02-002931>
- [29] Li, H., Li, Y., Yao, Q., Fan, J., Sun, W., Long, S., Shao, K., Du, J., Wang, J. and Peng, X. (2019) *In Situ* Imaging of Aminopeptidase N Activity in Hepatocellular Carcinoma: A Migration Model for Tumour Using an Activatable Two-Photon NIR Fluorescent Probe. *Chemical Science*, **10**, 1619-1625.
<https://doi.org/10.1039/C8SC04685A>
- [30] Hahnenkamp, A., Schafers, M., Bremer, C. and Holtke, C. (2013) Design and Synthesis of Small-Molecule Fluorescent Photoprobes Targeted to Aminopeptidase N (APN/CD13) for Optical Imaging of Angiogenesis. *Bioconjugate Chemistry*, **24**, 1027-1038. <https://doi.org/10.1021/bc400074w>